Relativistic Magnetic Reconnection in the Jets of High-Energy Peaked BL Lacertae Objects

Dr. Associate Prof. Bidzina Kapanadze

E. KharadzeNational Astrophysical Observatory (Abastumani, Georgia)

Space Research Center, Ilia State University (Tbilisi, Georgia)

INAF, Osservatorio Astronomico di Brera (Merate, Italy)

2023 October 23, Institut Astrophysique de Paris, France

BL Lacertae Objects

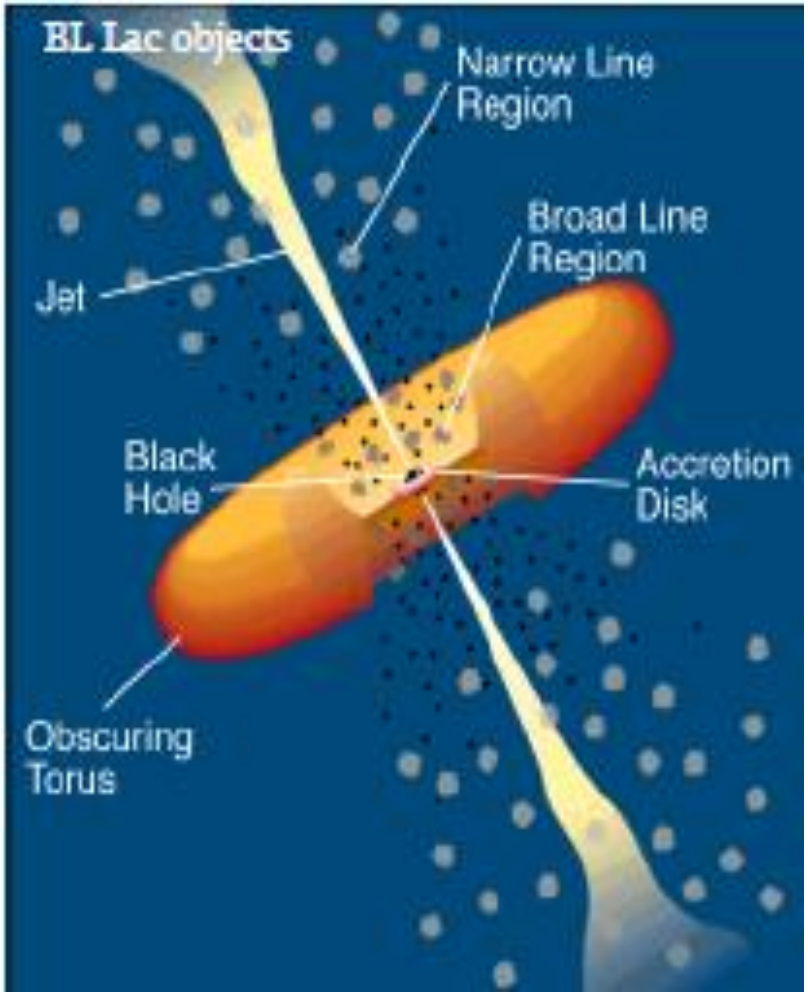

- BL Lacertae objects (BLLs, a blazar subclass)
  - AGNs of elliptical galaxies
  - Non-thermal continuum emission stretching from radio to TeV band (17-19 orders of frequency)
  - Absence of emission lines
  - Strong flux variability in all spectral bands
  - Compact and flat-spectrum radio emission
  - Apparent superluminal motion of some components
  - High and variable radio/optical polarization
  - Strong X-ray and γ-ray emissions: BLLs - a majority of extragalactic TeV sources and one of the most important constituent of Fermi-LAT catalogues
- Hypothetic structure: central supermassive BH (SMBH; 10^8-$10^9 M_{\odot}$) + acretion disc (AD) + two opposite jets (closely aligned to the observer)

- The best astrophysical sources in which our ideas on jet physics and particle acceleration can be tested are blazars

Particle Acceleration in BL Jets

- Key role to magnetic fields ➔ The energy stored in rapidly spinning Kerr SMBH extracted and channeled into Poynting flux (Blandford & Znajek 1977, Tchekhovskoy+ 2011)
- The jet power, originally carried by magnetically-dominated beam (with magnetization parameter $\sigma \equiv P_B/P_{kin} >> 1$) Progressively used to accelerate matter (≡ conversion from magnetic to kinetic energy), until a substantial equipartition between the magnetic and the kinetic energy fluxes ($\sigma \approx 1$) is established (Tchekhovskoy +2009) ➔
- Electrons (and, possibly, positrons and protons) should be accelerated to (utra)relativistic energies of TeV-order to produce X-ray - VHE photons (via synchrotron and IC mechanisms)
  - In the bulk frame of the electrons moving down the jet, for frequencies $\nu \sim 10^{17}$ Hz and B~0.1 G:
    - Radiative lifetimes of the order of one hour, corresponding to minutes in the observer's frame (assuming $\delta \sim 10$) ➔ The electron accelerated to ultra-relativistic energies by BZ-mechanism loose their energy, emitting X-ray photons (+ IC-scattering), very quickly
    - High keV-GeV states, observed on daily-weekly timescales, and X-ray emission detected at sub-pc, pc and sometimes at the kpc distances (Chandra observations; e.g. Marscher & Jorstad 2011): some local acceleration mechanisms in BLL jets to be continuously at work
  - Significantly higher X-ray luminosity during the flares than the maximal one expected from the initial acceleration

- Rapid TeV variability observed in BL Lacs (e.g. in PKS 2155−304 (Aharonian+2007) and Markarian 501 (Albert+2007)): time-scales of a few minutes ➔ Shorter, by at least an order of magnitude, than the light-crossing time of the central SMBH ➔

- *V*ariability is associated with small regions of the highly relativistic jet rather than the central region (light-travel argument)

- With the observed t_{var} *and* jet Lorentz factor Γ, the flare should occur at a distance greater than $c\, t_{var}\, \Gamma^2$ (Begelman+2008) ➔ Flaring region situated at the distance in excess of $100 r_s$ from the central SMBH ➔

- Charged particles are accelerated within the jet itself, close to the emission region via

  - ✓ *Magnetic reconnection*
  - ✓ Diffusive shock acceleration (DSA, first-oder Fermi-acceleration)
  - ✓ Stochastic (second-order Fermi) acceleration by magnetic turbulence in shocked jet area
  - ✓ …

Relativistic Magnetic Reconnection

- Magnetic reconnection: breaking and reconnecting of oppositely directed magnetic field lines in magnetized outflows ➔ Rapidly convert a sizeable magnetic energy into the particle kinetic energy via the rearrangement of the field lines

- Breaking ideal-MHD's frozen-in constraints & rearranging of the magnetic field topology ➔ Release of the free magnetic energy ➔ Converted into plasma kinetic and thermal energy

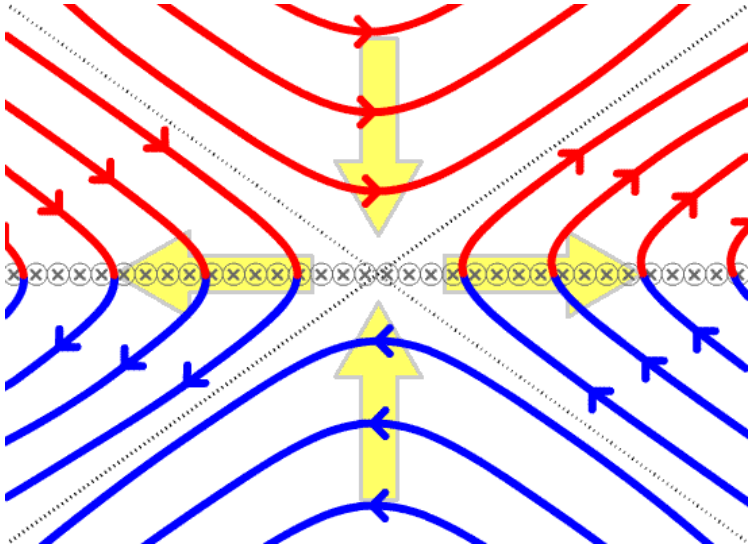

(https://upload.wikimedia.org/wikipedia/commons/2/24/Reconnection.gif?download)

- **Reconnection vs shocks** (Sol & Zech 2022)
  - ✓ Relativistic shocks convert only a fraction of the jet kinetic energy to accelerate charged particles
  - ✓ Magnetic reconnection -- rapid mechanism to directly use primary magnetic energy flux and accelerate particles to (ultra)relativistic energies

- Time evolution of the magnetic field in plasma

$$\delta \mathbf{B}/\delta t = \nabla \times (u \times \mathbf{B}) - \nabla \times \eta(\nabla \times \mathbf{B})$$

(u, typical plasma flow speed; η = c2/4$\pi\sigma$, magnetic diffusivity of the medium and σ, its conductivity)

- Astrophysical plasmas with high magnetic conductivity

  ✓ the first right-hand term is generally dominant ➔ Frozen-in magnetic field ➔ No reconnection

- Diffusive term can become dominant in various situations, e.g., when the first term dwindles to zero like around stagnation points, lines or surfaces with u ≃ 0 (Sol & Zech 2022) ➔

- Strong currents or current sheets with non-zero electric field induced ➔ Growing instabilities and turbulences induced by the currents ➔ Development of an anomalous resistivity ➔ Magnetic field destroyed and topology altered ➔ Magnetic reconnection (Uzdensky 2006,2011)

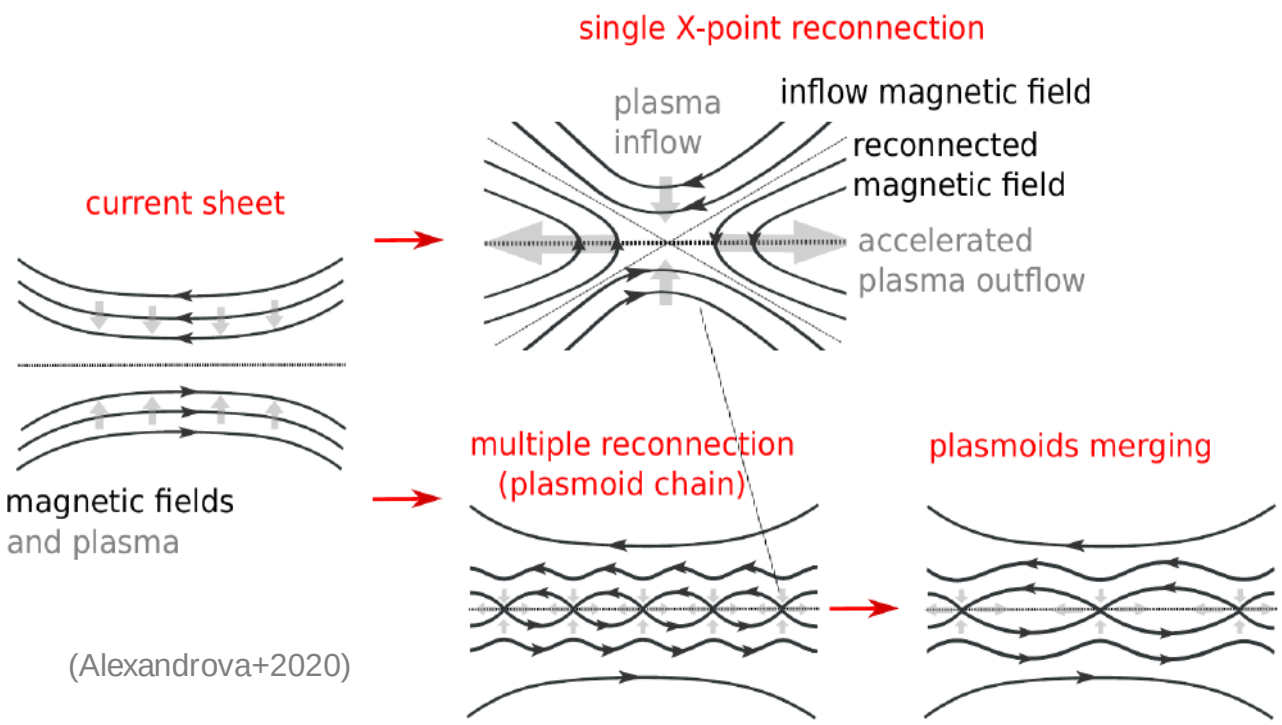

- In AGN jets, magnetic field lines can reverse on small scales due to (Zhang+2023)
  - ✓ nonlinear stages of MHD instabilities
  - ✓ jet can carry current sheets from its base
  - ✓ In both cases, field reversals on small scales are prone to magnetic reconnection
- Most reconnecting current sheets do not exhibit perfectly antialigned magnetic fields and a so-called guide present

- Reconnection matters when it results in a significant transfer of magnetic energy to gas ➔ **Transferred energy is larger than the internal in the gas before reconnection** ➔ Reconnection event to have a significant effect on the system only when the plasma is initially magnetically-dominated – magnetic to plasma internal energy ratio $\beta \ll 1$, i.e., when **the field is force-free** (Uzdensky 2006)
  - ✓ zero Lorentz force & magnetic pressure greatly exceeding the plasma pressure ➔
  - ✓ non-magnetic forces can be neglected
  - ✓ electric current density is either zero or parallel to the magnetic field

- Astrophysical jets: reconnection in the ``**relativistic**'' regime -- magnetic energy per particle can exceed the rest mass energy (Sironi & Spitkovsky 2014)

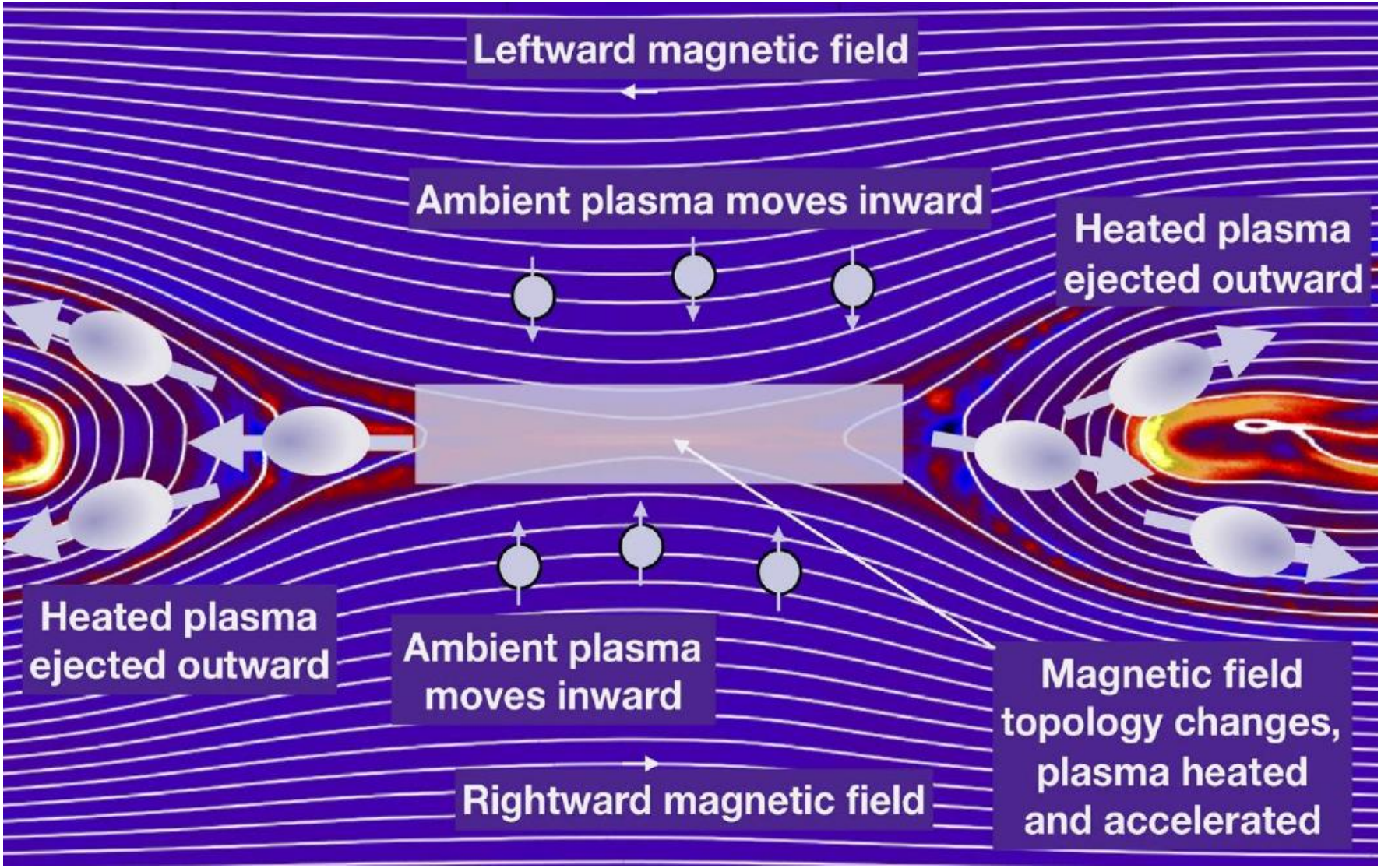

(Hesse & Cassak 2019)

- Two stages of downstream particle acceleration (French & Udzenky 2023):
  - ✓ Stage 1: pre-injection (or "pre-acceleration", "primary acceleration"; $\gamma \leq \gamma_{inj}$): particle energization from upstream thermal energy to the lower-energy boundary of the PL distribution
    - ➢ Direct acceleration by the reconnection electric field in magnetic X-points: occurs either in the initial current sheet or when two magnetic islands merge ➔ Magnetic field lines undergoing reconnection induce strong electric fields around the diffusion region ➔ Aaccelerate particles along the reconnected magnetic field in the case of a nonzero guide field
    - ➢ Fermi kick ("slingshot mechanism"): triggered by relaxation of freshly reconnected magnetic-field-line tension ➔ Curvature drift of particles:
      - ❑ Frst reflection by the curved field lines injects particles
      - ❑ After being kicked, the particle gains momentum mainly parallel to the local magnetic field (with the magnitude of the gain depending on Alfvén speed)

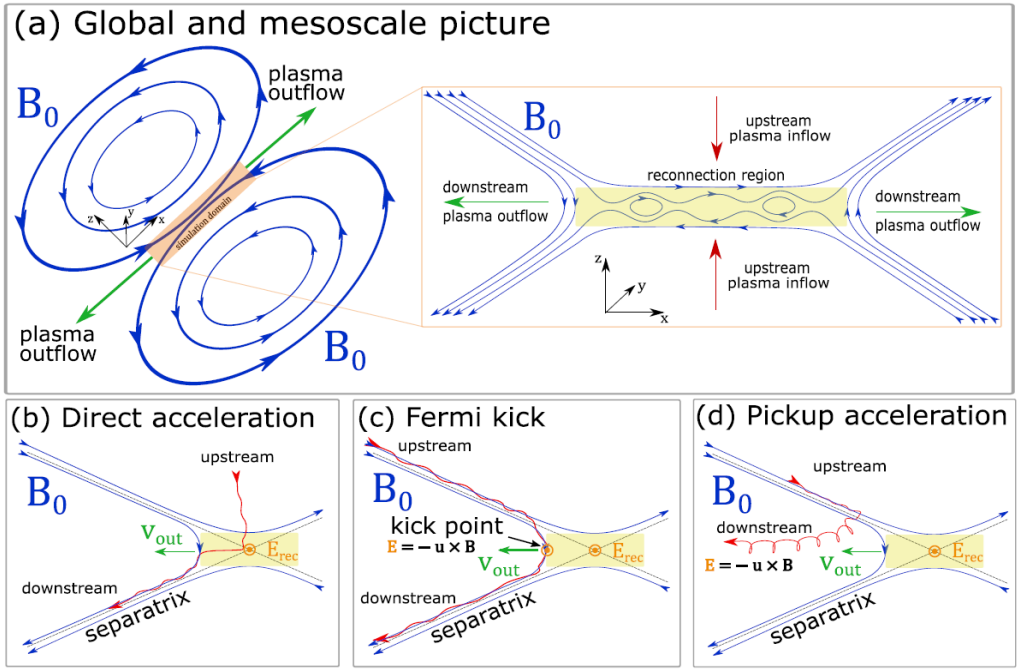

- ➢ Pickup acceleration (🡐 violation of magnetic moment adiabatic invariance): particle suddenly enters reconnection outflow region & Picked up" by the flow ➔ Rapid acceleration
- Fermi & pickup processes, related to the electric field perpendicular to the magnetic field, dominate within weak guide fields & larger domains
- Parallel electric fields: important within strong guide-field

(French & Udzenky 2023)

- Stage 2 ("post-injection", "secondary acceleration"): main energization stage -- high-energy acceleration ($\gamma \geq \gamma_{inj}$) ➔ Nonthermal PL distribution formed
  - ✓ Starts when the accelerating particles reach an energy sufficiently greater than the background upstream thermal energy
  - ✓ Weak and moderate guide fields: particle injection by perpendicular electric fields is more important (than that by parallel electric fields) ➔ Completely dominant in the high-energy (main) acceleration phase
  - ✓ Strong guide field can suppress acceleration processes related to perpendicular electric fields ➔ Parallel electric fields control acceleration

- Downstream electron spectrum: two components
  - ✓ Thermal -- Maxwellian-like distribution
  - ✓ High-energy nonthermal -- PL with a high-energy cutoff $f(\gamma) \propto \gamma^{-p} e^{-\frac{\gamma}{\gamma_c}}$
- *p*-index:
  - ✓ Related to the photon index (in the νFν representation)
  - ✓ $$\Gamma = (p+1)/2$$
  - ✓ Increases with domain l_x & guide-field strength $b_g = B_g/B_0$ (B_0, reconnecting magnetic field)
  - ✓ hardens with the upstream magnetzation $\sigma_h = B_0/4\pi h$ (≡ enthalpy density of the reconnecting magnetic field divided by the relativistic enthalpy density *h* of the upstream plasma):
    - ➢ For σ_h= 50, $p \sim 1.5$ to $p \sim 3.0$ depending on b_g (French & Uzdensky 2023)
    - ➢ Frequently harder than p=4 (in contrast to 4<p<1 for σ_h= 1!)
    - ➢ **Typically hard PL** ($p \gtrsim -2$) **established when** $\sigma_{up} \gtrsim 10$ (Sironi & Spitkovsky 2014)

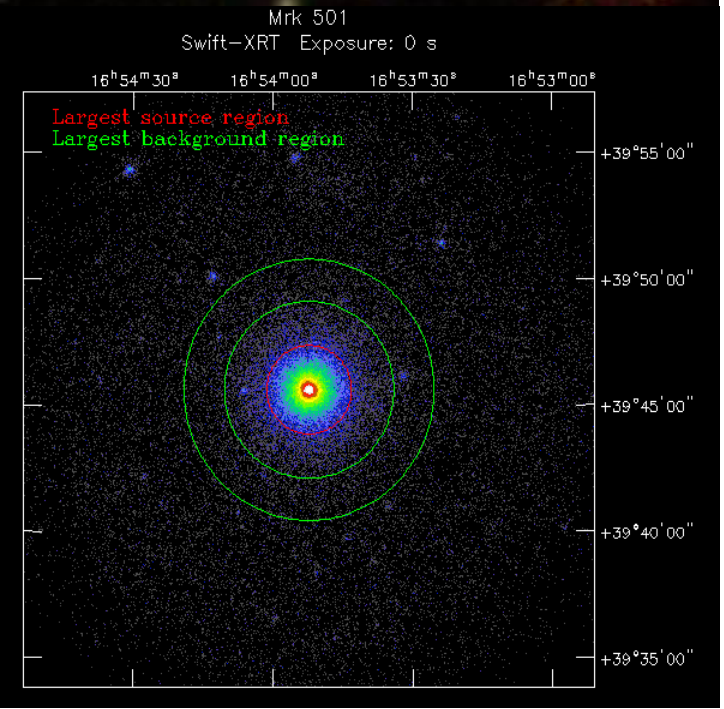

Mrk501

- R.A.:16 53 52.2 (hh mm ss)
- Dec.:+39 45 37 (dd mm ss)
- Redshift: z=0.034
- Distance: 456 Mly(140 Mpc)
- Bright X-ray source and the second extragalactic object detected in the TeVband (Quinn+1996)
- Central SMBH mass: $(0.9 - 3.4) \times 10^{10}\ M_{\odot}$
- Radio jet: 120 --200 kpc
- Intranight flux variability with flux-doubling times down to 2 minutes was observed with MAGIC during the two most active nights (2005 June 30 and July 9; Albert+2007)
- Variability by a factor of 30 with ~8 Crab during the dramatic TeV-band activity in 1997 March-October (Protheroe+1997) Meanwile, the synchrotron peak underwent a shift towards to energies of 100 keV (Pian+1998)
- The first source detected beyond 10 TeV, up to ~20 TeV(Aharonian+2001; "overwhelmed" only in 2019, by Crab making it the first identified source beyond 100 TeV)

- Mrk 501: **HBL source (synchrotron SED peak at UV—X-ray frequencies)**

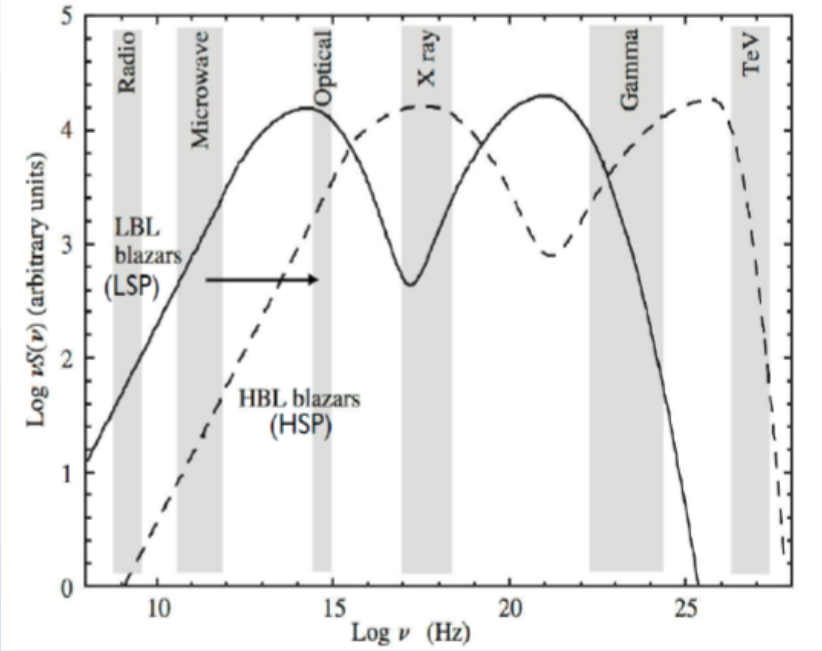

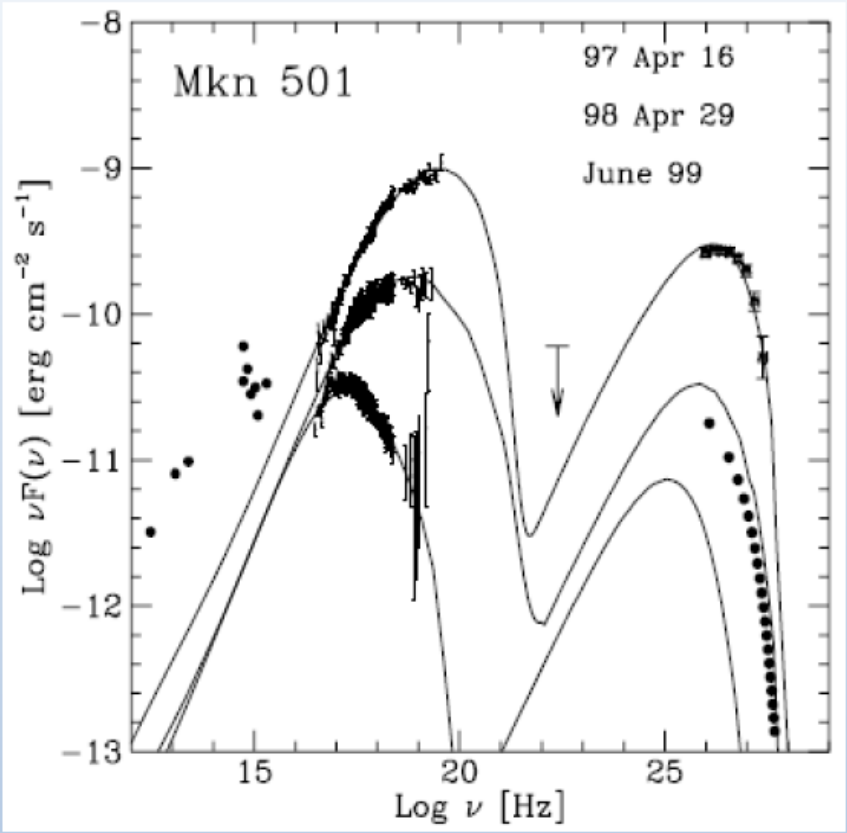

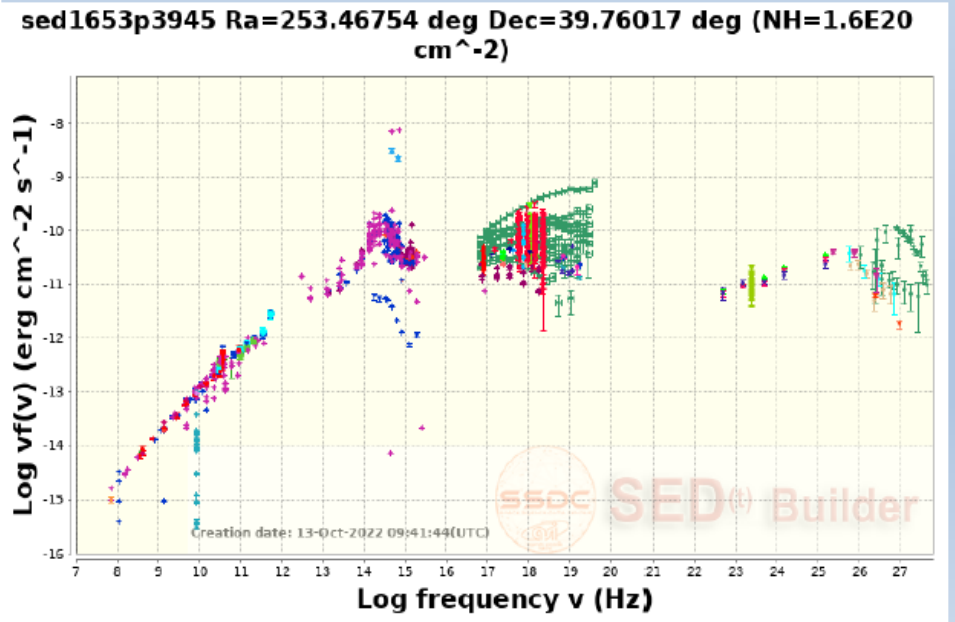

- Mrk 501: **frequent target for Swift-XRT**

Monthly Notices of the ROYAL ASTRONOMICAL SOCIETY

MNRAS **469**, 1655–1672 (2017) doi:10.1093/mnras/stx891
Advance Access publication 2017 April 17

The prolonged X-ray flaring activity of Mrk 501 in 2014

B. Kapanadze,[1,2★] D. Dorner,[3] P. Romano,[2] S. Vercellone,[2] K. Mannheim,[3] E. Lindfors,[4] K. Nilsson,[5] R. Reinthal,[4] L. Takalo,[4] S. Kapanadze[1] and L. Tabagari[1]

[1] *E. Kharadze Abastumani Astrophysical Observatory, Ilia State University, Colokashvili Av. 3/5, Tbilisi 0162, Georgia*
[2] *INAF, Osservatorio Astronomico di Brera, Via E. Bianchi 46, I-23807 Merate, Italy*
[3] *Institute for Theoretical Physics and Astrophysics, Universität Würzburg, Emil-Fischer-Str. 31, D-97074 Würzburg, Germany*
[4] *Tuorla Observatory, Department of Physics and Astronomy, University of Turku, FI-20014 Turku, Finland*
[5] *Finnish Centre for Astronomy with ESO (FINCA), University of Turku, Väisäläntie 20, FI-21500 Piikkiö, Finland*

Accepted 2017 April 7. Received 2017 April 7; in original form 2017 February 2

ABSTRACT

The X-ray variability of the BL Lacertae source Mrk 501 was studied during 11.5 yr of monitoring with *Swift*. Here, we report the results of this study pertaining to the epoch of 2014 March–October, when our target showed the most powerful and long-lasting X-ray flaring activity. This epoch was characterized by X-ray flares varying in amplitude by factors of 2–5 on time-scales of a few weeks or shorter. We detected 35 instances of the intraday variability, sometimes occurring within the 1 ks observational runs. The X-ray flux was generally correlated with the TeV flux, while the 0.3–300 GeV and optical-UV fluxes did not show a significant correlation. Some notable incidences of more complicated variability patterns could also be recognized, indicating that the high-energy emission in Mrk 501 arose from an emission region more complex than a single zone. The best fits of the 0.3–10 keV spectra were mainly obtained using the logparabola model. Strong spectral variability was detected, affecting the slope but not the curvature of the spectrum. In strong flares, the spectral index became harder than 1.70. The spectral evolution was characterized by a harder-when-brighter behaviour, shifting the peak of the spectral energy distribution by about 20 keV that happens rarely in blazars.

Key words: BL Lacertae objects: individual: Mrk 501.

The Astrophysical Journal Supplement Series, 268:20 (36pp), 2023 September https://doi.org/10.3847/1538-4365/ace69f

Long-term X-Ray Outburst in the TeV-detected Blazar Mrk 501 in 2021–2022: Further Clues for the Emission and Unstable Processes

B. Kapanadze[1,2,3], A. Gurchumelia[2,4], and M. Aller[5]
[1] Space Research Center, Department of Astronomy and Astrophysics, School of Natural Sciences and Medicine, Ilia State University, Colokashvili Av. 3/5, Tbilisi, 0162, Georgia; bidzina_kapanadze@iliauni.edu.ge
[2] E. Kharadze National Astrophysical Observatory, Mt. Kanobili, Abastumani, 0803, Georgia
[3] INAF, Osservatorio Astronomico di Brera, Via E. Bianchi 46, I-23807 Merate, Italy
[4] Department of Physics, I. Javaksishvili State University, Chavchavadze Av. 3, Tbilisi 012, Georgia
[5] Astronomy Department, University of Michigan, Ann Arbor, MI 48109-1107, USA
Received 2023 April 20; revised 2023 May 25; accepted 2023 June 20; published 2023 September 1

Abstract

This paper presents the results of a detailed X-ray timing and spectral analysis of Mrk 501, which are based mainly on the Swift data obtained during 2021 February–2022 December. The source showed strongly enhanced X-ray activity, characterized by a long-term increase in the baseline 0.3–10 keV flux level superimposed by shorter-term flares on timescales of a few weeks to about 2 months. During some time intervals, Mrk 501 was the brightest blazar in the X-ray sky and, moreover, showed an intense intraday variability, which was sometimes detected within the exposures lasting a few hundred seconds. These instances were characterized by fractional variability amplitudes of 4%–18% and were mostly observed during short-term X-ray flares. The source exhibited extreme spectral properties with dominance of the spectral curvature, frequent occurrence of hard photon indices in the 0.3–10 keV and 0.3–300 GeV bands, and the peak of a synchrotron spectral energy distribution in the hard X-ray range. These properties demonstrate the importance of relativistic magnetic reconnection, first-order Fermi mechanism within the magnetic field of different confinement efficiencies, stochastic acceleration, and hadronic processes. The X-ray and γ-ray fluxes showed a log-normal distribution, which hints at the imprint of accretion disk instabilities on the blazar jet, as well as the possible presence of hadronic cascades and random fluctuations in the particle acceleration rate. The optical–UV and γ-ray variabilities showed a weak or absent correlation with the X-ray flaring activity, which is not consistent with simple leptonic models and requires more complex particle acceleration, emission, and variability scenarios.

- Mak 501: Frequent occurrence of hard 0.3-10 keV and 0.3-300 GeV powerlaw (PL) photon index

(Kapanadze+2023)

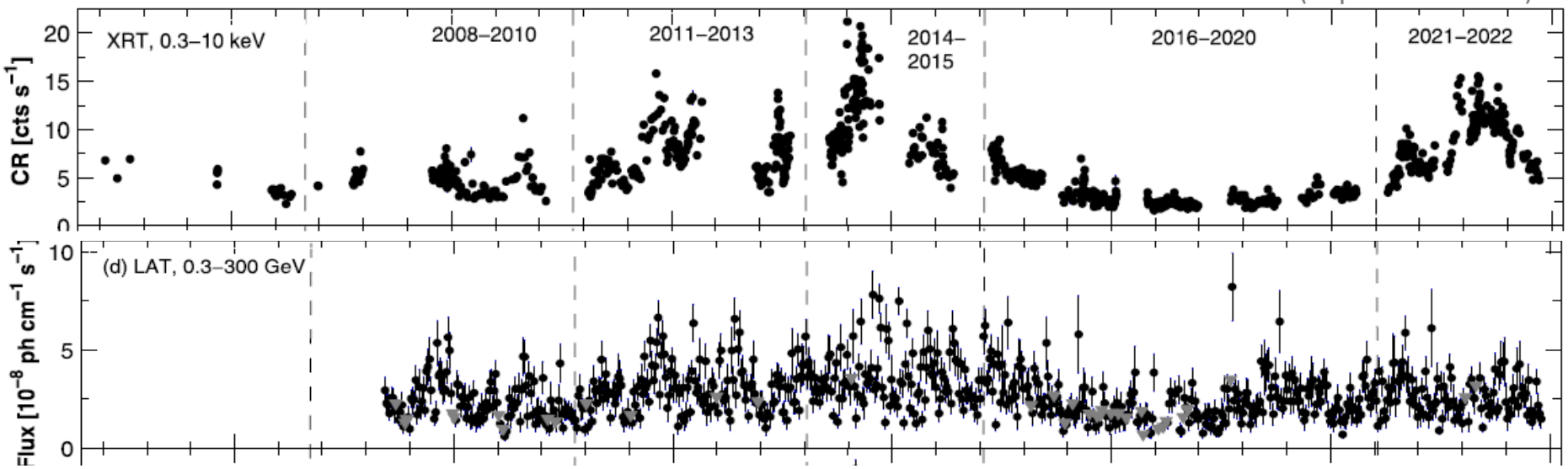

0.3-10 keV

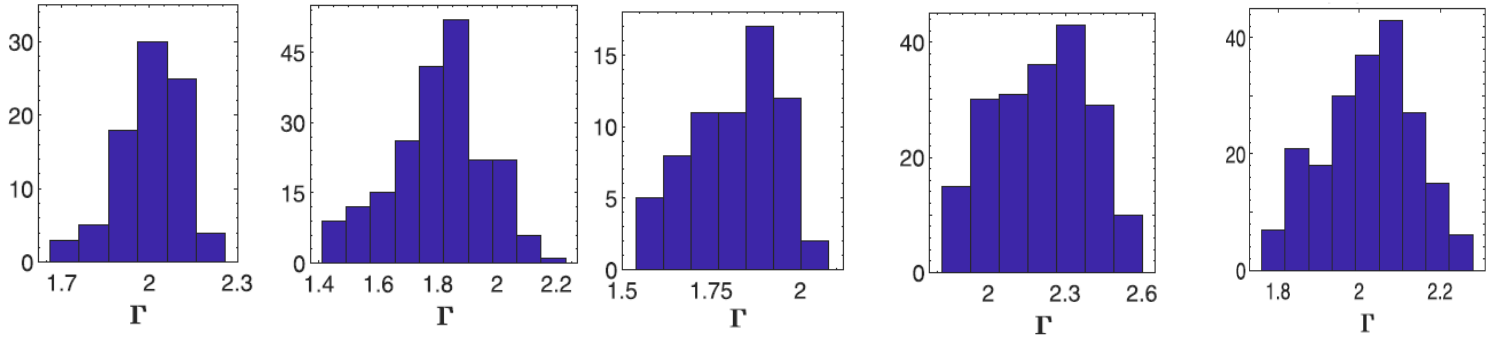

0.3-300 GeV

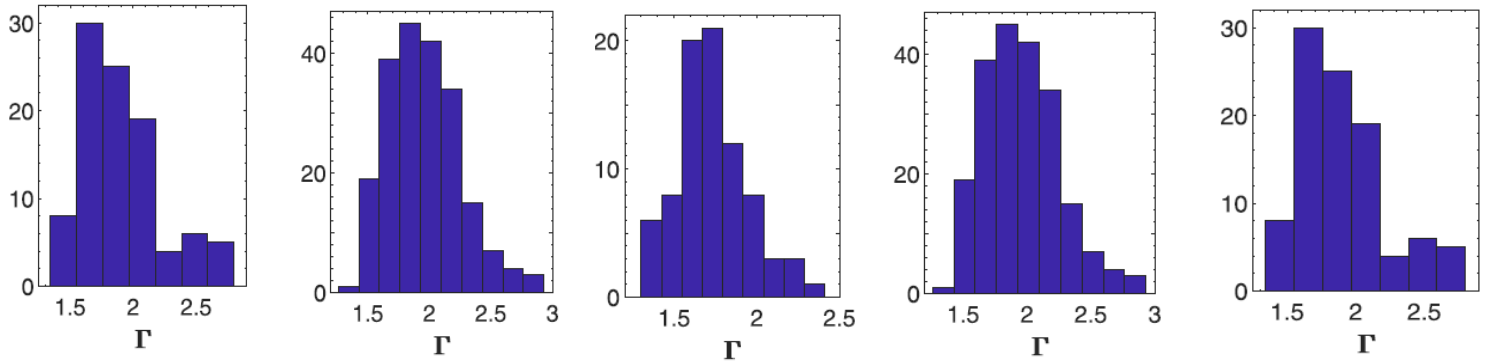

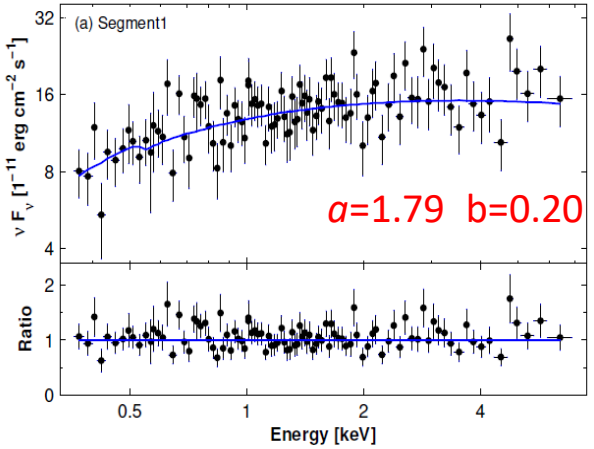

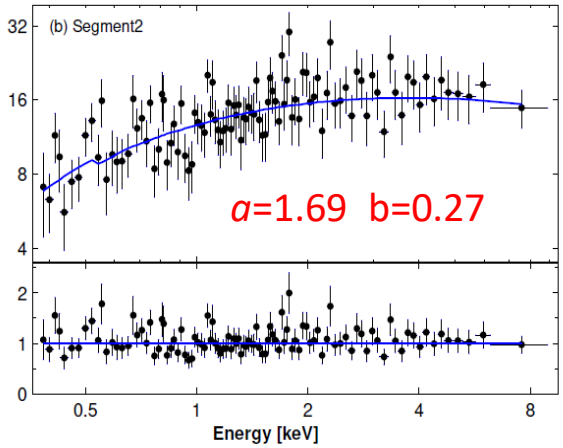

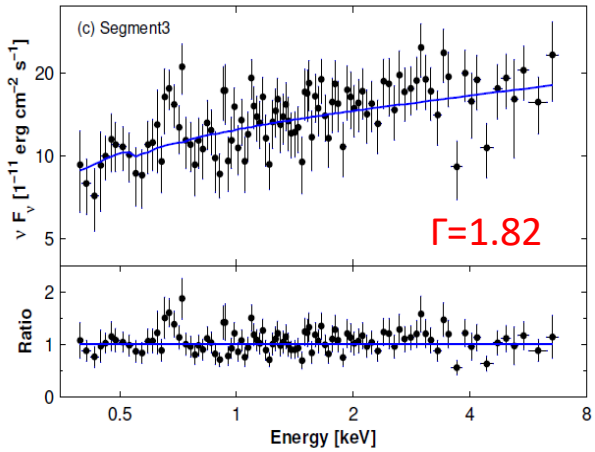

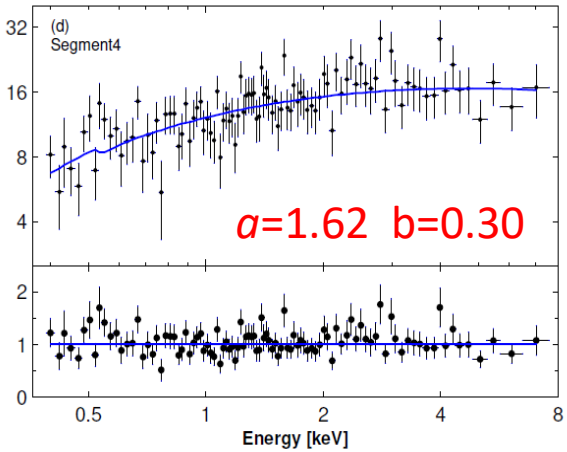

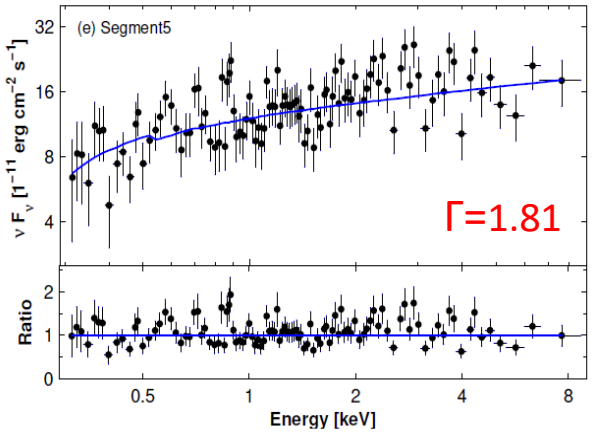

- Extreme 0.3-10 keV spectral variability of Mrk 501 : transition from the log-parabolic into a power-law spectrum and vice versa, within 1 ks observational run

✓ Spectra from each 195-sec segment of ObsID 11184188:

➢ Logparabolic model in Panels (a), (b) and (d) with low curvature characteristic for stochastic (Fermi II)acceleration

➢ Hard PL spectra in Panels (c) and (e) – plausibly established by relativistic magnetic reconnection (Kapanadze+2023)

- Changes in the particle acceleration mechanism on spatial sclales of $\sim 10^{12}$cm (for typical Lorentz factor of the emission zone $\Gamma_{em} = 10$ (Falomo et al. 2014) ➔
- **Turbullence-driven relativistic magnetic reconnection** - the most plausible explanation for the hard PL spectra
- Frequent occurrence of such extremely fast transitions in some periods, frequently associated with flux variability

Swift-XRT Observations of Mrk 501: Period 2011—2013

- **ObsID 11184188** S2(195s) LP a=1.69(0.04) b=0.27 (0.09) ➔ S3(195s) PL Γ=1.82(0.03) ➔ S4(325s) LP a=1.63(0.04) b=0.29 (0.09) ➔ S5(195s) PL Γ=1.81(0.03)
- **ObsID 30793197** S1(365s) LP a= 1.64(0.04) b=0.15(0.08 ➔ S2 (365s) PL Γ=1.75(0.03) ➔ S3(365s) LP a= 1.65(0.04) b=0.16(0.08) ➔ S4 (365s) PL Γ=1.71(0.03)
- **ObsID 11184191** S2(305s) LP a=1.84(0.04) b=0.21 (0.07) ➔ S3(305s) PL Γ=1.96(0.03) ➔ S4(305s) LP a=1.88(0.05) b=0.19 (0.08) ➔ S5(305s) PL Γ=1.89(0.03)
- **ObsID 11184189** S1(335s) PL Γ=1.82(0.03) ➔ S2(335s) LP a=1.71(0.04) b=0.19 (0.07) ➔ S3(335s) LP a=1.67(0.04) b=0.30 (0.08) ➔ S4(335s) PL Γ=1.80(0.03) ➔ S5(335s) LP a=1.71(0.04) b=0.30(0.08)
- **ObsID 11184194** S1(300s) LP a=1.86(0.04) b=0.17 (0.08) ➔ S2(300s) PL Γ=1.97(0.03) ➔ S3(3000s) LP a=1.91(0.04) b=0.32 (0.08) ➔ S4(300s) PL Γ=1.94(0.03)
- **ObsID 30793036** S2(295s) LP a= 1.47(0.04) b=0.21(0.07) ➔ S3(295s) PL Γ=1.58(0.03) ➔ S4(295s) LP a= 1.53(0.04) b=0.16 (0.07)
- **ObsID30793039** S1(455s) PL Γ=1.65(0.03) ➔ S2 (455s) LP a= 1.63(0.04) b=0.17 (0.07) ➔ S3 (455s) PL Γ=1.65(0.03)
- **ObsID 307930143** S2(255s) LP a= 1.52(0.04) b=0.19(0.08) ➔ S3(255s) PL Γ=1.58(0.03) ➔ S4(255s) LP a= 1.59(0.04) b=0.17(0.07)
- **ObsID 91745009** S2(325s) PL Γ=1.81(0.03) ➔ S3(325s) LP a=2.03(0.04) b=0.15 (0.07) ➔ S4 PL Γ=1.73(0.03)
- **ObsID30793234** S1(240s) LP a= 1.69(0.04) b=0.26(0.21) ➔ S2(240s) PL Γ=1.78(0.03) ➔ S3(240s) PL Γ=1.84 (0.03) ➔ S4(240s) LP a= 1.69(0.04) b=0.26(0.08)

- **ObsID91745004** S1 LP a= 1.57(0.05) *b*=0.27(0.08) ➔ S2 PL Γ=1.66(0.03) ➔ S3 LP a= 1.54(0.05) *b*=0.20(0.08)
- **ObsID30793148** S1(250s) PL Γ=1.72(0.03) ➔ S2(250s) LP a= 1.67(0.04) *b*=0.15 (0.07) ➔ S3(250s) PL Γ=1.72(0.03)
- **ObsID30793188** S1(235s) LP a= 1.67(0.04) *b*=0.12 (0.06) ➔ S2(235s) PL Γ=1.71(0.03) ➔ S3(235s) PL Γ=1.73(0.03) ➔ S4(235s) PL Γ=1.70(0.03)
- **ObsID30793142** S2(285s) LP a= 1.48(0.05) *b*=0.21(0.08) ➔ S3(285s) PL Γ=1.57(0.03) ➔ S4(235s) PL Γ=1.62(0.03)
- **ObsID30793235** S1(240s) PL Γ=1.72(0.03) ➔ S2(240s) PL Γ=1.79(0.03) ➔ S3(240s) LP *a*=1.71(0.04) *b*=0.21 (0.08)
- **ObsID30793236** S3(255s) LP a= 1.63(0.04) *b*=0.22(0.08) ➔ S4(255s) PL Γ=1.75(0.03) ➔ S5(255s) PL Γ=1.70(0.03)
- **ObsID30793241** S1(385s) LP a= 1.73(0.04) *b*=0.13(0.06) ➔ S2(385s) PL Γ=1.78(0.03) ➔ S3(385s) PL Γ=1.76(0.03)
- **ObsID91745008** S1 LP a= 1.33(0.04) *b*=0.18(0.07) ➔ S2 PL Γ=1.70(0.03) ➔ S3 PL Γ=1.67(0.03)
- **ObsID91745023** S2 LP a= 1.67(0.04) *b*=0.16(0.08) ➔S3 PL Γ=1.81(0.03) ➔ S4 PL Γ=1.75(0.03)
- **ObsID11184231** ➔ S1(275s) PL Γ=2.07(0.03) ➔ S2(275s) LP *a*=2.03(0.04) *b*=0.16 (0.07) ➔ S3(275s) PL Γ=2.02(0.03)
- **ObsID11184225** S1(320s) PL Γ=2.12(0.03) ➔ S2(320s) LP *a*=2.03(0.04) *b*=0.15 (0.07)➔ S3(320s) PL Γ=2.09(0.03)
- **ObsID11184222** S1(320s) PL Γ=2.12(0.03) ➔ S2(320s) LP *a*=2.03(0.04) *b*=0.15 (0.07) ➔ S3(320s) PL Γ=2.09(0.03)

- **ObsID96558007** S1(250s) PL Γ=2.10(0.03) ➔ S2(250s) LP *a*=2.1.92(0.05) *b*=0.44 (0.11) ➔ S3(250s) PL Γ=2.10 (0.03)
- **ObsID91745019** S1(320s) LP a= 1.60(0.04) *b*=0.22(0.08) ➔ S2(320s) PL Γ=1.75(0.03) ➔ S3(320s) PL Γ=1.72(0.03)
- **ObsID96558003** S2(320s) LP *a*=1.89(0.04) *b*=0.2415 (0.08) ➔S3(345s) PL Γ=1.96(0.03) ➔ S4(345s) PL Γ=2.02(0.03)
- **ObsID30793233** S2(340s) LP a= 1.62(0.04) *b*=0.28(0.08) ➔ S3(340s) PL Γ=1.76(0.03)
- **ObsID30793235** S1(240s) LP a= 1.72(0.03) *b*=0.16(0.06) ➔ S2(240s) PL Γ=1.79(0.02)
- **ObsID30793238** S2(540s) LP a= 1.70(0.04) *b*=0.17(0.08) ➔ S3(540s) PL Γ=1.77(0.03)
- **ObsID30793238** Or1 S2(350s) LP a= 1.77(0.04) *b*=0.18(0.08) ➔ S2(350s) PL Γ=1.85(0.03)
- **ObsID91745005** Or2 S1(310s) LP a= 1.46(0.05) *b*=0.19(0.10) ➔ S2(310s) PL Γ=1.59(0.04)
- **ObsID30793145** S1(280s) PL Γ=1.71(0.03) ➔ S2(280s) LP a= 1.63(0.04) *b*=0.17(0.07)
- **ObsID30793146** S2(250s) PL Γ=1.65(0.03) ➔ S3(250s) LP *a*=1.55(0.04) *b*=0.23 (0.07
- **ObsID30793047** S2(270s) LP a= 1.61(0.04) *b*=0.24(0.08) ➔ S3(270s) PL Γ=1.71(0.03)
- **ObsID30793165** S1(310s) PL Γ=1.75(0.03) (310s) ➔ S2(310s) LP *a*=1.66(0.04) *b*=0.18(0.08)
- **ObsID30793166** S1(330s) PL Γ=1.76(0.03) ➔ S2(330s) LP *a*=1.69(0.04) *b*=0.18 (0.07)
- **ObsID30793188** S1(310s) LP a= 1.74(0.04) *b*=0.12 (0.06) ➔ S2(310s) PL Γ=1.80(0.03)
- **ObsID30793173** S1 (340s) PL Γ=1.73(0.03) ➔ S2(340s) LP *a*=1.57(0.04) *b*=0.20 (0.08)
- **ObsID30793188** S1(310s) LP a= 1.73(0.04) *b*=0.12 (0.06) ➔ S2(310s) PL Γ=1.75(0.03)
- **ObsID30793197** S1(365s) LP a= 1.58(0.04) *b*=0.21(0.07) ➔ S2(365s) PL Γ=1.72(0.02)
- **ObsID30793200** S1(380s) PL Γ=1.71(0.03) ➔ S2(380s) LP *a*=1.57(0.04) *b*=0.20 (0.08)

Mergers Between Large Plasmoids

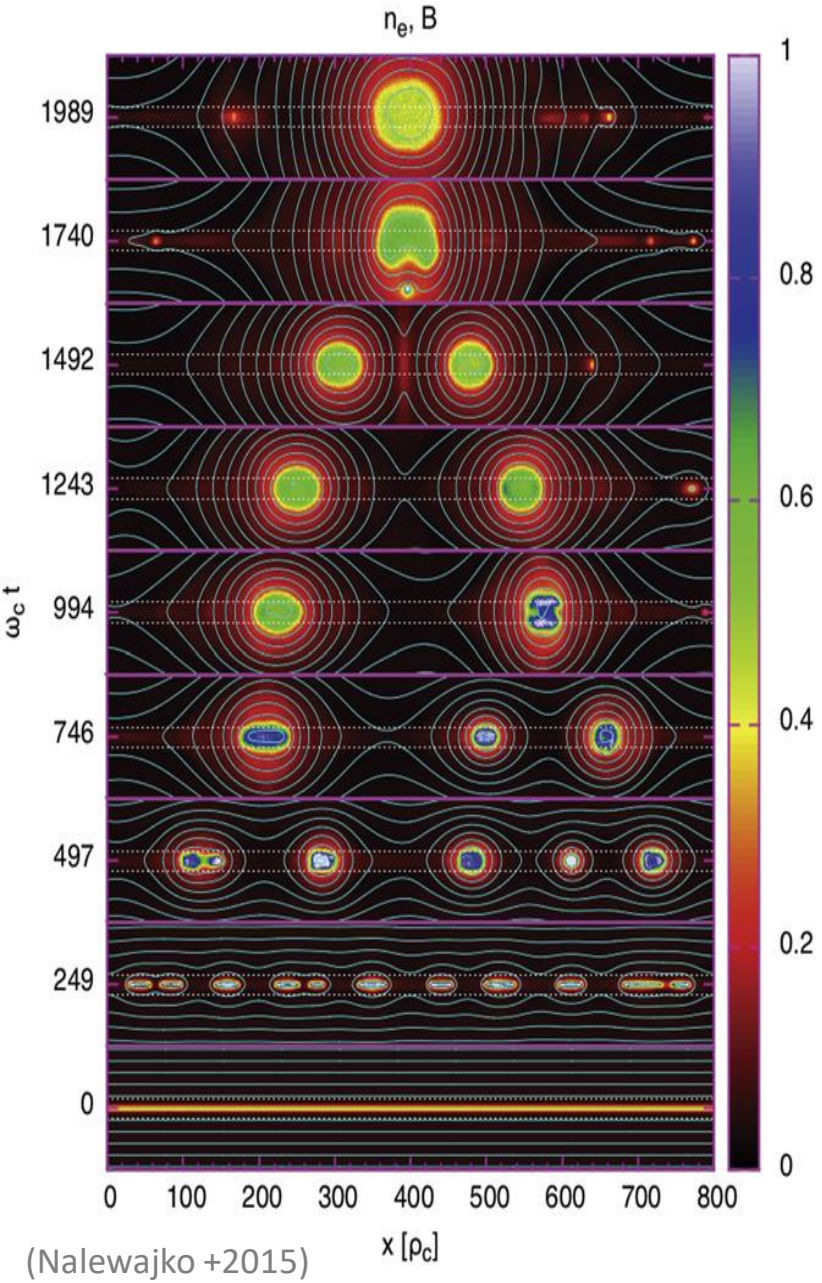

(Nalewajko +2015)

- Fast magnetic reconnection (2-D simulation;
  Hakobyan+2021; Nalewajko+2015)
  - ✓Self-similar chain of plasmoids formed
  - ✓Each plasmoid
    - ➢ accumulate particles both from the adjacent current sheets
    - ➢ grow in time
    - ➢ compress interior and amplify the internal magnetic field linearly with time ➔
    - ➢ Energize particles due to magnetic moment conservation ➔
  - ✓**Adding a nonthermal tail $f(E) \propto E^{-3}$ to the existing powerlaw EED at higher energies**, followed by an exponential cutoff
  - ✓ **Cutoff energy increases with time**

$$E_{\rm cut} \propto \sqrt{t},$$

  - ➢ Extremely large values achieved depending on the process duration ➔
  - ➢ **Filling the EED's highest-energy tail with particles capable of producing the Swift-BAT-band emission in HBLs** (synchrotron mechanism)

- Large plasmoids mergers:
  - ✓ Possibly most important for Mrk 501 in 2005–2006 and 2011–2014 ➔
  - ✓ relatively frequent BAT-band detections with 5σ and strong 15—150 keV flares

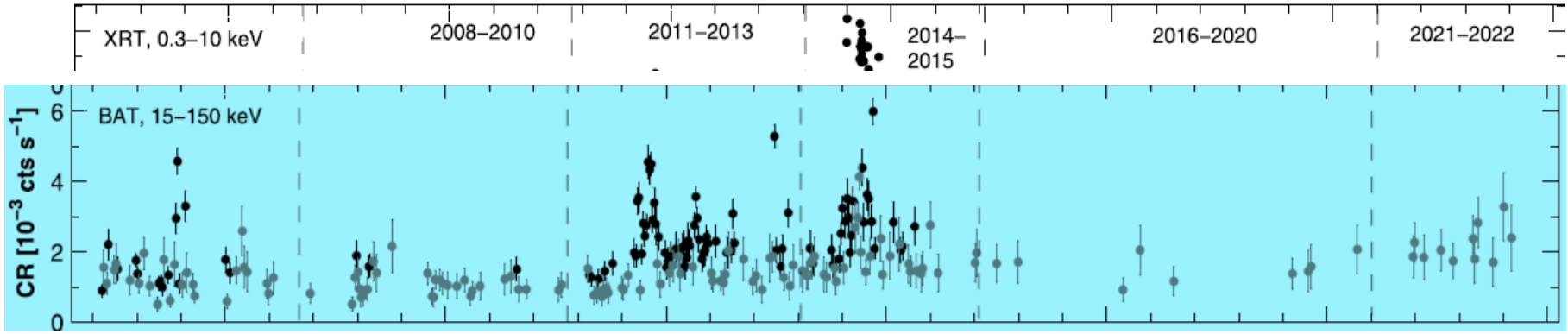

- 3-D Case (Zhang+2021):
  - ✓ Fraction of particles can "break free" from plasmoids by moving along z-axis and then experience the large-scale motional electric field in the upstream region
  - ✓ Accelerated linearly with time ($\gamma \propto t$) while undergoing Fermi I-like deflections by converging upstream flows – faster than during large plasmoid mergers
  - ✓ Net very hard PL spectrum $f(\gamma) \propto \gamma^{-1.5}$ for $\sigma_{up} \gtrsim 10$
  - ✓ "Free" particles may account for $\sim$ 20% of the dissipated magnetic energy, independently of domain size
  - ✓ Seems to be relatively less important for Mrk 501

Mrk 421

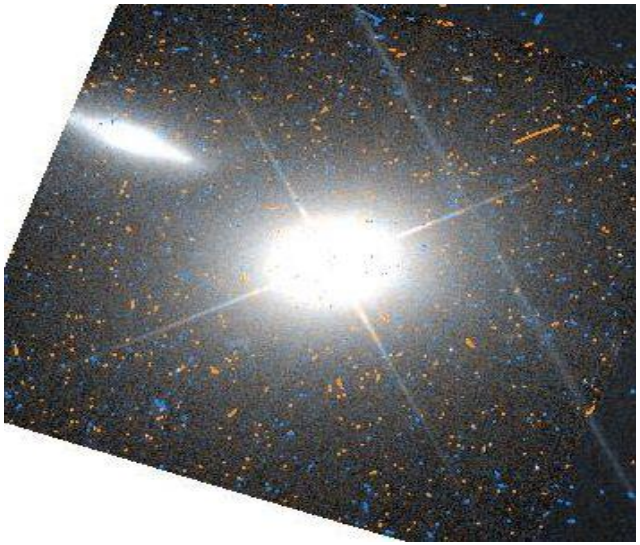

HST optical image (Scarpa+2000)

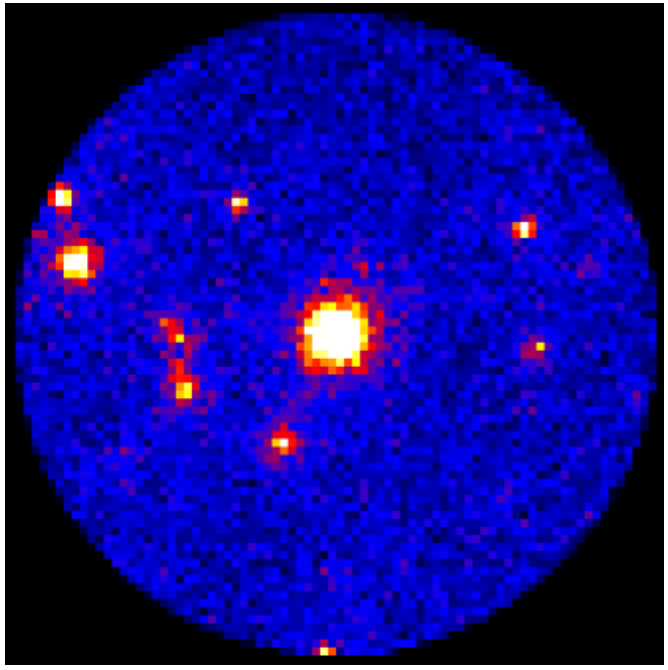

0.3-300 GeV image

- Active nucleus of bright elliptical galaxy with effective radius of 6.64 kpc (Wu+2000)
- HBL source situated at z=0.031
- The first extragalactic TeV-detected source (Punch +1992), and regularly observed in this energy range afterwards (Gaidos+1996, Aharonian+1999, 2002, 2003,2005,2007; Acciari+2009,2011,2014; Aielli+2010; Aleksic+2010,2012, 2015a,2015b; Bartoli+2011,2016; Balokovic+2016 etc.)
- Highest-energy photon with E >10 TeV (Okomura+2002)
- Extreme VHE flux variability (e.g. Gaiodos+1996)
- The brightest HBL in the 0.3—10 keV and 0.3--300 GeV bands
- **My "favorite" target** (2020ApJS..247...27K, 2019hepr.confE..15K, 2018ApJ...858...68K, 2018ApJ...854...66K, 2017ApJ...848..103K, 2017AIPC.1792e0021K, 2016ApJ...831..102K, 2016frap.confE..33K, 2014ies..conf..116K Atels#16062,9137, 7654, 4918, 4864, 4792)

Swift-XRT Observations of Mrk 421: Period 2005—2008

- **ID30352011** **Or1** S1(200s) PL Γ=1.88(0.01) ➔ S2(200s) LP *a*= 1.84(0.02) *b*=0.10(0.04) ➔.... ➔ S4 (200s) LP *a*= 1.86(0.02) *b*=0.10(0.04) ➔ S5(230s) PL Γ=1.89(0.01) ➔ ... ➔ **Or2** S2(200s) LP *a*= 1.86(0.02) *b*=0.10(0.04) ➔ S3(300s) PL Γ=1.88(0.02) ➔ ... ➔ **Or3** S6(200s) LP *a*= 1.87(0.02) *b*=0.16(0.04) ➔ S7(130s) PL Γ=1.91(0.02) ➔ ... ... ➔ **Or4** S4(200s) LP *a*= 1.98(0.04) *b*=0.09(0.04) ➔ S5(250s) PL Γ=2.03(0.01) ➔ S6(270s) LP *a*= 1.97(0.02) *b*=0.11(0.04) ➔ ... ➔ **Or7** S1(260s) LP *a*= 2.02(0.02) *b*=0.08(0.04) ➔ S2(250s) PL Γ=2.03(0.01) ➔ ... ➔ **Or10** S1(250s) PL Γ=1.93(0.01) ➔ S2(270s) LP *a*= 2.02(0.04) *b*=0.09(0.04) ➔ S3(250s) PL Γ=1.96(0.01) ➔ S4(200s) LP *a*=2.04(0.04) *b*=0.12(0.04) ➔ S5(250s) PL Γ=1.96(0.01) ➔ S6(260s) LP *a*=2.09(0.01) *b*=0.09(0.04) ➔ S7(200s) PL Γ=1.98(0.01) ➔ .... **Or11** S1(240s) LP *a*= 1.91(0.02) *b*=0.10(0.04) ➔ S2(240s) PL Γ=1.95(0.01) ➔... ➔ **Or13** S2(250s) PL Γ=1.91(0.01) ➔ S3(250s) LP *a*= 1.92(0.02) *b*=0.10(0.04) ➔ **Or14** S1(250s) PL Γ=1.95(0.01) ➔ S2(250s) LP *a*= 1.90(0.02) *b*=0.12(0.04) ➔ S3(250s) PL Γ=1.92(0.01) ➔ **Or15** S2(270s) LP *a*= 1.94(0.02) *b*=0.13(0.04) ➔ S3(270s) PL Γ=2.02(0.01) ➔ **Or16** S1(250s) LP *a*= 1.98(0.02) *b*=0.12(0.04) ➔ S2(250s) PL Γ=2.05(0.02) ➔ ... ➔ **Or19** S3(250s) LP *a*= 1.95(0.02) *b*=0.10(0.04) ➔ S4(310s) PL Γ=1.96(0.01) ➔ **Or20** S1(250s) LP *a*= 1.92(0.02) *b*=0.0.08(0.04) ➔ S2(250s) PL Γ=1.94(0.01) ➔ S3(250s) LP *a*= 1.94(0.02) *b*=0.0.08(0.04) ➔ S4(260s) PL Γ=1.96(0.01) ➔ ... **Or21** S3(250s) LP *a*= 1.97(0.02) *b*=0.11(0.04) ➔ S4(310s) PL Γ=1.98(0.01) ➔ **Or22** S2(350s) LP *a*= 2.00(0.02) *b*=0.0.08(0.04) ➔ S3(300s) PL Γ=2.05(0.02) ➔ **Or23** S1(360s) PL Γ=2.08(0.01) ➔ S2(360s) LP *a*= 2.03(0.02) *b*=0.08(0.04) ➔ ... **Or25** S1(340s) LP *a*= 2.07(0.02) *b*=0.11(0.04) ➔ S2(340s) PL Γ=2.08(0.01) ➔ ... ➔ **Or30** S1(250s) LP *a*= 1.85(0.02) *b*=0.11(0.04) ➔ S2(250s) PL Γ=1.88(0.01) ➔ S3(250s) LP *a*= 1.89(0.02) *b*=0.12(0.04) ➔ ... ➔ **Or31** S1(250s) PL Γ=1.89(0.01) ➔ S2(250s) LP *a*= 1.89(0.04) *b*=0.09(0.09) ➔ S3(300s) PL Γ=1.90(0.01) ➔ S4(285s) LP *a*=2.04(0.04) *b*=0.12(0.04) ➔ ... ➔ **Or33** S1(240s) LP *a*= 1.86(0.02) *b*=0.09(0.04) ➔ S2(240s) PL Γ=1.90(0.02)

- **ID30352015** **Or1** S1(200s) PL Γ=1.92(0.01) ➔ S2(200s) LP *a*= 1.86(0.02) *b*=0.08(0.04) ➔ S3(250s) PL Γ=1.88(0.01) ➔ **Or2** S1(235s) PL Γ=1.87(0.01) ➔ S2(140s) LP *a*= 1.91(0.02) *b*=0.11(0.04) ➔ … ➔ **Or4** S1(200s) LP *a*= 1.88(0.02) *b*=0.09(0.04) ➔ S2(150s) PL Γ=1.88(0.01) ➔ S3(200s) PL Γ=1.90(0.01) ➔ S4(140s) LP *a*= 1.86(0.02) *b*=0.0.08(0.04) ➔ S5(200s) PL Γ=1.90(0.01) ➔ **Or5** S2(200s) LP *a*= 1.88(0.02) *b*=0.14(0.04) ➔ S3(200s) PL Γ=1.91(0.01) ➔ S4(200s) LP *a*= 1.91(0.02) *b*=0.08(0.04) ➔ S5(150s) PL Γ=1.93(0.01) ➔… ➔ **Or6** S2(170s) LP *a*= 1.84(0.02) *b*=0.14(0.04) ➔ S3(140s) PL Γ=1.85(0.01) ➔ … ➔ **Or7** S2(220s) LP *a*= 1.82(0.02) *b*=0.09(0.03) ➔ S3(220s) PL Γ=1.88(0.01) ➔ … ➔ **Or8** S2(210s) LP *a*= 1.82(0.02) *b*=0.12(0.03) ➔ S3(210s) PL Γ=1.88(0.01) ➔… … ➔ **Or9** S3(210s) LP *a*= 1.92(0.02) *b*=0.08(0.03) ➔ S4(210s) PL Γ=1.96(0.01) ➔ **Or10** S1(200s) PL Γ=1.98(0.01) ➔ S2(200s) LP *a*= 1.93(0.02) *b*=0.10(0.03) ➔ S3(250s) PL Γ=1.96(0.01) ➔ S4(250s) LP *a*= 1.98(0.02) *b*=0.08(0.03) ➔ **Or11** S1(200s) LP *a*= 1.95(0.02) *b*=0.11(0.03) ➔ S2(200s) PL Γ=1.2.01(0.01) ➔ S3(150s) LP *a*= 1.96(0.02) *b*=0.13(0.03) S1(200s) ➔ S4(200s) LP *a*=2.01(0.02) *b*=0.09(0.04) ➔ S5(150s) PL Γ=2.01(0.02) ➔ **Or12** S2(200s) PL Γ=1.99(0.01) ➔ S3(150s) LP *a*= 1.95(0.02) *b*=0.08(0.04) ➔ S4(200s) LP *a*=1.98(0.02) *b*=0.08(0.04) ➔ S5(160s) PL Γ=2.00(0.02) ➔ … ➔ **Or13** S2(200s) LP *a*= 1.97(0.02) *b*=0.08(0.03) ➔ S3(200s) PL Γ=1.990.01) ➔ … ➔ **Or15** S1(200s) PL Γ=1.2.02(0.01) ➔ S2(2000s) LP *a*= 2.01(0.02) *b*=0.08(0.04) ➔S3(200s) LP *a*=2.03(0.02) *b*=0.08(0.04) ➔ S4(160s) PL Γ=2.05(0.02)

- **ID30352014** **Or7** S2 (180s) PL Γ=1.74(0.01) ➔ S3(140s) LP *a*= 1.73(0.02) *b*=0.10(0.04) ➔ S4(180s) PL Γ=1.77(0.02) ➔… ➔ **Or8** S2(180s) PL Γ=1.84(0.01) ➔ S3(190s) LP *a*= 1.80(0.02) *b*=0.08(0.04) ➔ S4(180s) PL Γ=1.84(0.01) ➔… ➔ **Or9** S1(180s) LP *a*= 1.82(0.02) *b*=0.08(0.04) ➔ S2(180s) PL Γ=1.84(0.01) ➔… ➔ **Or7** S2 (180s) PL Γ=1.86(0.01) ➔ S3(180s) LP *a*= 1.86(0.02) *b*=0.08(0.04) ➔ S4(180s) PL Γ=1.87(0.02)

ID30352010 **Or1** S3(250s) PL Γ=1.97(0.02) ➔ S4(250s) LP *a*= 1.98(0.02) *b*=0.12(0.04) ➔ S5(230s) PL Γ=1.99(0.02) ➔ **Or2** S1(250s) LP *a*= 1.89(0.02) *b*=0.10(0.04) ➔ S2(250s) PL Γ=1.91(0.02) ➔ …➔ S4(150s) PL Γ=1.90(0.02) ➔ S5(250s) LP *a*= 1.88(0.02) *b*=0.16(0.04) ➔ … ➔ **Or3** S2(250s) LP *a*= 1.90(0.02) *b*=0.11(0.04) ➔ S3(250s) PL Γ=1.93(0.02) ➔ S4(250s) LP *a*= 1.88(0.02) *b*=0.09(0.04) ➔ S5(250s) PL Γ=1.90(0.02) ➔… ➔ **Or4** S2(250s) LP *a*= 1.89(0.02) *b*=0.09(0.04) ➔ S3(250s) PL Γ=1.92(0.02) ➔ S4(250s) PL Γ=1.88(0.02) ➔… ➔ **Or5** S1(250s) PL Γ=1.86(0.02) ➔ S2(300s) LP *a*= 1.83(0.02) *b*=0.10(0.04) ➔ S3(250s) PL Γ=1.88(0.02) ➔ S4(250s) LP *a*= 1.84(0.02) *b*=0.09(0.04) ➔ S5(290s) PL Γ=1.85(0.01) ➔… ➔ **Or6** S2(200s) PL Γ=1.85(0.01) ➔ S3(250s) LP *a*= 1.82(0.02) *b*=0.08(0.04) ➔ S4(250s) PL Γ=1.83(0.01) ➔ S5(320s) PL Γ=1.86(0.01) ➔ … ➔ **Or14** S1(250s) LP *a*= 1.76(0.02) *b*=0.09(0.04) ➔ S2(300s) PL Γ=1.79(0.01) ➔ … ➔ … ➔ **Or15** S1(250s) PL Γ=1.85(0.01) ➔ S2(300s) LP *a*= 1.79(0.02) *b*=0.09(0.04) ➔ S3(250s) PL Γ=1.81(0.01) ➔ S4(250s) PL Γ=1.84(0.01) ➔ … ➔ **Or16** S1(150s) LP *a*= 1.81(0.03) *b*=0.12(0.05) ➔ S2(150s) PL Γ=1.88(0.02) ➔ … ➔ **Or17** S3(250s) PL Γ=1.84(0.01) ➔ S4(250s) LP *a*= 1.81(0.02) *b*=0.11(0.04) ➔ S5(150s) PL Γ=1.82(0.01) ➔ **Or23** S3(240s) PL Γ=1.84(0.01) ➔ S4(240s) LP *a*= 1.78(0.02) *b*=0.09(0.04) ➔ ➔ S5(250s) PL Γ=1.80(0.01)

ID206476000 **Or1** S1(265s) LP *a*= 1.73(0.02) *b*=0.12(0.04) ➔ S2(265s) PL Γ=1.77(0.02) ➔ .. ➔ **Or4** S1(220s) LP *a*= 1.74(0.02) *b*=0.12(0.04) ➔ S2(220s) PL Γ=1.75(0.01) ➔ .. ➔ **Or14** S1(220s) LP *a*= 1.82(0.02) *b*=0.11(0.04) ➔ S2(220s) PL Γ=1.85(0.02) ➔ **Or15** S1(240s) LP *a*= 1.89(0.02) *b*=0.10(0.04) ➔ S2(205s) PL Γ=1.88(0.02)

ID30352013 **Or2** S4(250s) LP *a*= 1.99(0.02) *b*=0.14(0.04) ➔ S5(250s) PL Γ=2.03(0.02) ➔ **Or5** S1(250s) LP *a*= 2.02(0.02) *b*=0.08(0.04) ➔ S2(250s) PL Γ=2.09(0.02) ➔ S3(250s) LP *a*= 2.08(0.02) *b*=0.08(0.04) ➔ … ➔ **Or6** S1(250s) LP *a*=1.99(0.02) *b*=0.15(0.04) ➔ S2(250s) PL Γ=2.03(0.02) ➔ S3(250s) LP *a*= 2.03(0.02) *b*=0.10(0.04) ➔ S4(250s) PL Γ=2.07(0.02) ➔… **Or7** S2(300s) PL Γ=1.99(0.01) ➔ S3(300s) LP *a*= 1.99(0.02) *b*=0.08(0.04) ➔ S4(300s) PL Γ=1.98(0.01) ➔ … ➔ **Or10** S2(250s) PL Γ=1.85(0.02) ➔ S3(250s) LP *a*= 1.88(0.02) *b*=0.09(0.04) ➔ S4(300s) PL Γ=1.90(0.01) ➔ S5(300s) LP *a*= 1.85(0.02) *b*=0.08(0.04) ➔ … ➔ **Or15** S2(300s) LP *a*= 1.94(0.02) *b*=0.09(0.04) ➔ S3(300s) PL Γ=1.97(0.01) ➔ S4(250s) PL Γ=1.95(0.01) ➔ S5(300s) LP *a*= 1.93(0.02) *b*=0.08(0.04)

Mini-Jet Model

- Based on relativistic magnetic reconnection (Giannios+2009)
  - ✓ Two wedge-shape regions with relativistically flowing plasma ("mini-jets") and separated by a stationary shock
  - ✓ Mini-jets:
    - ➢ perpendicular to the relativistic jet axis
    - ➢ formed in the process of magnetic reconnection
    - ➢ moving with relativistic speeds
    - ➢ produce fastly variably TeV-emission within a narrow beam via SSC mechanism
- Multiple, reconnection-born mini-jets: adopted to explain the subsequent very fast TeV-flares in PKS 2155-304 in 2006 July

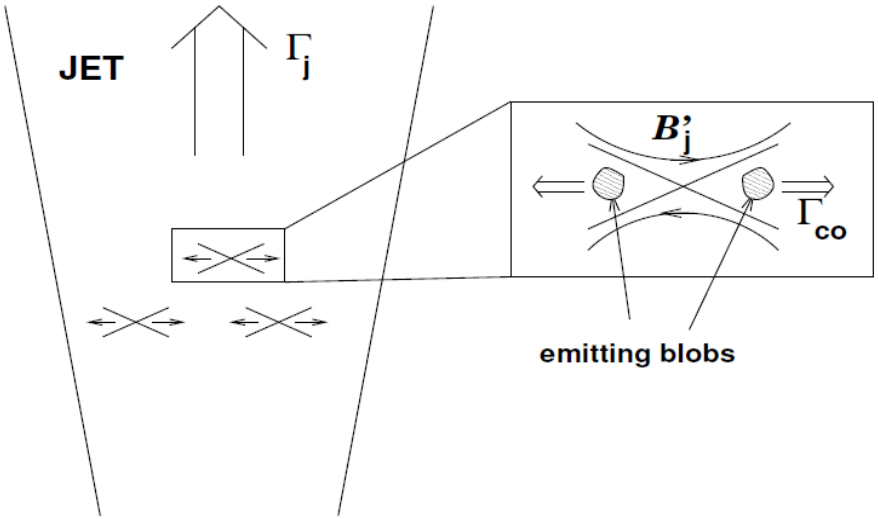

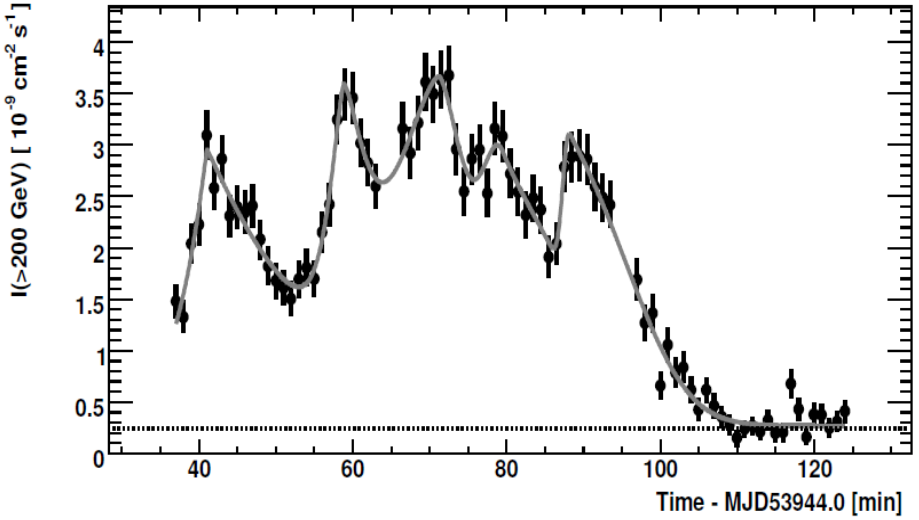

Conclusions and Future Plans

- **HBLs – one of the most extreme particle accelerators in the universe**
  - ✓ Bright sources in the 0.3-10 keV energy range ➔ Spectral variability can be detected within a few hundred seconds ➔ injection and radiative evolution of freshly accelerated particles can be tracked ➔ Draw conclusions about particle Acceleration mechanisms
  - ✓ Extreme 0.3-10 keV spectral variability in Mrk 421 and 501: transition from the log-parabolic into a power-law spectrum and vice versa, within 1 ks observational run (over spatial scales $\sim 10^{12} - 10^{13}$ cm)
    - ➢ Turbulence-driven relativistic magnetic reconnection: the most plausible mechanism for establishing the PL spectra!
    - ➢ The PL photon index $\Gamma \sim 1.4—2.4$ in 0.3-10 keV band ➔ Particle index $p \sim 1.8—3.8$ ➔ Large variety of the upstream magnetization and/or guide-field strength and/or reconnection area size
    - ➢ However, rare occurrence of the upstream magnetization $\sigma_{up} \gtrsim 10$: ➔ $p < 2$ ➔ $\Gamma < 1.5$
    - ➢ Even harder p-values from Fermi-LAT data (SSC model): $\Gamma \sim 1.4—2.4$ in 0.3—300 GeV
      - ❑ Caution: possible hadronic contribution? (also capable to produce hard spectra) ➔ SED modeling required (reconnection-based and leptohadronic) ➔
      - ❑ Construct broadband SEDs for the particular time intervals and fit with the different emission scanrios (including the hadronic models to be most suitable for HBLs); adopt the particle EED established in the presence of relativistic magnetic reconnection
- Very fast LP→PL/PL→LP transitions are not found for some X-ray bright HBLs, e.g. 1ES 1959+650:
  - ✓ General LP spectra and rare occurrence of PL PED
  - ✓ However, recent detection additional H_2 content ➔ Increase of the total absorption column density by $\sim 60\%$ (to 1.63×10^{21}) ➔ Significantly higher possibility to detect PL spectra and very fast LP→PL/PL→LP transitions

Acknowledgements

Thanks to

- Shota Rustaveli National Science Foundation and E. Kharadze National Astrophysical Observatory (Abastumani, Georgia) for the fundamental research grant FR−21−307, providing with a financial support to participate in the workshop
- Workshop organizers for the invitation and hospitality